

# Near-threshold $\eta'$ meson production in $\pi^-A$ reactions

E. Ya. Paryev<sup>1,2</sup>

<sup>1</sup>*Institute for Nuclear Research, Russian Academy of Sciences,  
Moscow 117312, Russia*

<sup>2</sup>*Institute for Theoretical and Experimental Physics,  
Moscow 117218, Russia*

## Abstract

We study the inclusive near-threshold production of  $\eta'$  mesons in  $\pi^-$  meson-nucleus reactions on the basis of the first-collision model relying on the nuclear spectral function and including incoherent processes of  $\eta'$  production in  $\pi^-$  meson-proton collisions. The model accounts for the absorption of initial  $\pi^-$  and final  $\eta'$  mesons, the binding of intranuclear protons and their Fermi motion, as well as the effect of the scalar  $\eta'$ -nucleus potential (or the in-medium shift of the  $\eta'$  meson mass) on these processes. We calculate the differential and total cross sections for  $\eta'$  production off carbon and tungsten nuclei at laboratory angles of  $0^\circ$ – $10^\circ$  and  $10^\circ$ – $45^\circ$  by  $\pi^-$  mesons with momentum of 1.7 GeV/c, which is close to the threshold momentum for  $\eta'$  creation on a free target proton at rest. We show that the calculated  $\eta'$  production cross sections are larger than those, studied earlier in the  $\eta'$  photoproduction reactions, by about two orders of magnitude. We also demonstrate that the high absolute values of the present differential and total  $\eta'$  production cross sections in the momentum ranges of 0.2–0.3 GeV/c and 0.1–0.6 GeV/c, respectively, possess a high sensitivity to changes in the in-medium shift of the  $\eta'$  mass. This offers the possibility of evaluating the above shift at these momenta from the respective data, which could be taken in future experiments at the GSI pion beam facility or at J-PARC.

# 1 Introduction

Studies of the  $\eta'$  meson mass and its interaction in finite nuclei have received considerable interest in recent years due to the hope to extract valuable information on the partial restoration of chiral symmetry at finite density, on gluon dynamics in low-energy QCD, and on the possible formation of  $\eta'$  bound states inside the nuclei (see, for example, Refs. [1, 2]). Recent measurements of inclusive  $\eta'$  photoproduction from carbon [3] and niobium [4] nuclear targets by the CBELSA/TAPS Collaboration in Bonn gave for the real part  $V_0$  of the  $\eta'$ -nucleus potential at saturation density  $\rho_0$  (which is equal to the  $\eta'$  meson mass shift in the medium) the combined value of  $V_0 = -(39 \pm 7_{stat} \pm 15_{syst})$  MeV [1, 4] for average momentum of the produced  $\eta'$  of  $\approx 1.1$  GeV/c. A new determination of the  $\eta'$ -nucleus potential  $V_0$  with lower average  $\eta'$  momentum of 600 MeV/c was performed also by the CBELSA/TAPS Collaboration [5] by measuring the production of  $\eta'$  mesons in coincidence with forward-going protons in photon-induced reactions on  $^{12}\text{C}$  for initial photon energies of 1.3–2.6 GeV at the electron accelerator ELSA with the result  $V_0 = -(44 \pm 16_{stat} \pm 15_{syst})$  MeV, consistent with the above value for the potential  $V_0$ , deduced from inclusive measurements for average  $\eta'$  momentum of  $\approx 1.1$  GeV/c. The imaginary part  $W_0$  of the  $\eta'$ -nucleus optical potential was determined in [6] to be  $W_0 = -(13 \pm 3_{stat} \pm 3_{syst})$  MeV near-threshold from an extrapolation of the transparency ratio measurements on Nb at various  $\eta'$  momenta well above threshold to near-threshold momenta. These numbers, with a small modulus of the imaginary  $\eta'$  meson potential compared to the modulus of its real potential suggest that  $\eta'$ -nucleus bound states may exist, provided that the above relation between the imaginary and real potentials persists at low  $\eta'$  momenta as well. Thus, the knowledge of the real part of the  $\eta'$ -nucleus potential for meson momenta small compared to its mass is crucial for understanding the feasibility of forthcoming experiments aiming at the search for  $\eta'$  mesic bound states. The search of such states in the  $^{12}\text{C}(p, d)$  reaction near the  $\eta'$  emission threshold has been recently undertaken at FRS/GSI [7]. No distinct structures, associated with the formation of  $\eta'$  bound states, were observed. In the near future, the search of  $\eta'$  mesic nuclei is also planned at GSI/FAIR [7] as well as in photonuclear reactions at ELSA [8].

In the context of aforesaid, it is interesting to consider another reactions such as  $\pi^- A \rightarrow \eta' X$  for clarifying the possibility of constraining in them the  $\eta'$  meson real potential at low momenta. In this respect, the main purpose of the present work is to give the predictions for the differential and total cross sections for  $\eta'$  production in  $\pi^- ^{12}\text{C} \rightarrow \eta' X$  and  $\pi^- ^{184}\text{W} \rightarrow \eta' X$  reactions at 1.7 GeV/c beam momentum. These nuclear targets and this initial momentum were employed in recent measurements [9] of  $\pi^-$  meson-induced  $\phi$  meson production at the GSI pion beam facility [10] and, therefore, can be used in studying the  $\pi^- A \rightarrow \eta' X$  reactions again at GSI or at J-PARC <sup>1)</sup>. The calculations are based on a first-collision model, developed in [13] for the analysis of the inclusive  $\phi$  meson production data [9] and expanded to take into account different scenarios for the  $\eta'$  meson in-medium mass shift. When the respective data from the future experiments will become available, the results can be used as an important tool for determining this shift at low meson momenta.

---

<sup>1)</sup>Especially in view of the fact that there are proposals at J-PARC which plan to use the  $(\pi^-, n)$  reaction on nuclear targets to look for  $\eta$  [11] and  $\omega$  [12] bound states in nuclei.

## 2 Framework: a direct $\eta'$ meson knock out process

The direct production of  $\eta'$  mesons in  $\pi^- A$  ( $A = {}^{12}\text{C}$  and  ${}^{184}\text{W}$ ) collisions at incident momentum of 1.7 GeV/c can occur in the following  $\pi^- p$  elementary process with zero pions in the final state <sup>2)</sup>

$$\pi^- + p \rightarrow \eta' + n. \quad (1)$$

Following Ref. [14], we simplify the subsequent calculations via accounting for in-medium modification of  $\eta'$  mesons, involved in process (1), in terms of their average in-medium mass  $\langle m_{\eta'}^* \rangle$ , which is defined as:

$$\langle m_{\eta'}^* \rangle = m_{\eta'} + V_0 \frac{\langle \rho_N \rangle}{\rho_0}. \quad (2)$$

Here,  $m_{\eta'}$  is the  $\eta'$  rest mass in free space,  $V_0$  is the  $\eta'$  effective scalar nuclear potential (or its in-medium mass shift) at normal nuclear matter density  $\rho_0$ , and  $\langle \rho_N \rangle$  is the average nucleon density. For target nuclei  ${}^{12}\text{C}$  and  ${}^{184}\text{W}$ , the ratio  $\langle \rho_N \rangle / \rho_0$ , was chosen as 0.55 and 0.76, respectively, in our ensuing study. The total energy  $E'_{\eta'}$  of the  $\eta'$  meson in nuclear matter is expressed via its average effective mass  $\langle m_{\eta'}^* \rangle$  and its in-medium momentum  $\mathbf{p}'_{\eta'}$  by the equation [14]:

$$E'_{\eta'} = \sqrt{(\mathbf{p}'_{\eta'})^2 + (\langle m_{\eta'}^* \rangle)^2}. \quad (3)$$

The momentum  $\mathbf{p}'_{\eta'}$  is related to the vacuum  $\eta'$  momentum  $\mathbf{p}_{\eta'}$  as follows [14]:

$$E'_{\eta'} = \sqrt{(\mathbf{p}'_{\eta'})^2 + (\langle m_{\eta'}^* \rangle)^2} = \sqrt{\mathbf{p}_{\eta'}^2 + m_{\eta'}^2} = E_{\eta'}, \quad (4)$$

where  $E_{\eta'}$  is the  $\eta'$  total energy in vacuum.

As indicated above, the potential depth  $V_0$  of about -40 MeV was deduced in semi-exclusive [5] and inclusive [3, 4]  $\eta'$  photoproduction experiments for average  $\eta'$  momenta of 0.6 and 1.1 GeV/c, respectively. Therefore, in this work it is natural to use the value  $V_0 = -40$  MeV for the  $\eta'$  mass shift  $V_0$  at density  $\rho_0$  for all studied  $\eta'$  momenta. In order to see the sensitivity of the  $\eta'$  production cross sections from the process (1) to the  $\eta'$  mass shift  $V_0$ , we will also both ignore it in our calculations and will adopt the value  $V_0 = -80$  MeV, predicted by the linear sigma model [15]. It should be pointed out that we restrict ourselves to the above values for the potential depth  $V_0$  due to the fact that strongly attractive potentials  $V_0 \leq -100$  MeV were excluded (for a relatively shallow imaginary potentials) by the experiment of Tanaka et al. [7] (see, also [1]). For the sake of numerical simplicity, in the present work in evaluating the  $\eta'$  production cross sections we will disregard the modification of the mass of the neutrons, produced together with the  $\eta'$  mesons in reaction channel (1), in the nuclear mean field [16].

Because the  $\eta'$ -nucleon elastic cross section is expected to be small [17], we will neglect quasielastic  $\eta'N$  rescatterings in the present study. Then, taking into consideration the distortion of the incident pion in nuclear matter and describing the  $\eta'$  meson final-state absorption by the effective in-medium momentum-independent  $\eta'N$  inelastic cross section  $\sigma_{\eta'N}$  <sup>3)</sup> as well as using the results

<sup>2)</sup>The free threshold momentum for this process is 1.43 GeV/c. We can ignore the processes  $\pi^- N \rightarrow \eta' N \pi$  with one pion in the final state at the incident momentum of interest, because this momentum is less than their production threshold momenta in free  $\pi^- N$  interactions. Thus, for example, the threshold momentum of the channel  $\pi^- p \rightarrow \eta' n \pi^0$  is 1.72 GeV/c. This momentum is larger than the incident pion momentum of 1.7 GeV/c. Consequently, the processes  $\pi^- N \rightarrow \eta' N \pi$  are energetically suppressed. Moreover, accounting for the results of the study [13] of pion-induced  $\phi$  meson production on  ${}^{12}\text{C}$  and  ${}^{184}\text{W}$  target nuclei at pion beam momentum of 1.7 GeV/c, we neglect in the present work by analogy with [13] the secondary pion-nucleon  $\pi N \rightarrow \eta' N$  production processes.

<sup>3)</sup>For this cross section we adopt the value  $\sigma_{\eta'N} = 13$  mb motivated by the results from the  $\eta'$  photoproduction CBELSA/TAPS experiment [6].

presented in Ref. [13], we represent the inclusive differential cross section for the production of  $\eta'$  mesons with vacuum momentum  $\mathbf{p}_{\eta'}$  on nuclei in the direct process (1) as follows:

$$\frac{d\sigma_{\pi^- A \rightarrow \eta' X}^{(\text{prim})}(\mathbf{p}_{\pi^-}, \mathbf{p}_{\eta'})}{d\mathbf{p}_{\eta'}} = I_V[A, \theta_{\eta'}] \left( \frac{Z}{A} \right) \left\langle \frac{d\sigma_{\pi^- p \rightarrow \eta' n}(\mathbf{p}_{\pi^-}, \mathbf{p}_{\eta'})}{d\mathbf{p}_{\eta'}} \right\rangle_A \frac{d\mathbf{p}_{\eta'}}{d\mathbf{p}_{\eta'}}, \quad (5)$$

where

$$I_V[A, \theta_{\eta'}] = A \int_0^R r_{\perp} dr_{\perp} \int_{-\sqrt{R^2 - r_{\perp}^2}}^{\sqrt{R^2 - r_{\perp}^2}} dz \rho(\sqrt{r_{\perp}^2 + z^2}) \exp \left[ -\sigma_{\pi^- N}^{\text{tot}} A \int_{-\sqrt{R^2 - r_{\perp}^2}}^z \rho(\sqrt{r_{\perp}^2 + x^2}) dx \right] \quad (6)$$

$$\times \int_0^{2\pi} d\varphi \exp \left[ -\sigma_{\eta' N} A \int_0^{l(\theta_{\eta'}, \varphi)} \rho(\sqrt{x^2 + 2a(\theta_{\eta'}, \varphi)x + b + R^2}) dx \right], \quad (7)$$

$$l(\theta_{\eta'}, \varphi) = \sqrt{a^2(\theta_{\eta'}, \varphi) - b - a(\theta_{\eta'}, \varphi)}, \quad (8)$$

$$\left\langle \frac{d\sigma_{\pi^- p \rightarrow \eta' n}(\mathbf{p}_{\pi^-}, \mathbf{p}_{\eta'})}{d\mathbf{p}_{\eta'}} \right\rangle_A = \int \int P_A(\mathbf{p}_t, E) d\mathbf{p}_t dE \quad (9)$$

$$\times \left\{ \frac{d\sigma_{\pi^- p \rightarrow \eta' n}[\sqrt{s}, < m_{\eta'}^*, >, m_n, \mathbf{p}_{\eta'}]}{d\mathbf{p}_{\eta'}} \right\}$$

and

$$s = (E_{\pi^-} + E_t)^2 - (\mathbf{p}_{\pi^-} + \mathbf{p}_t)^2, \quad (10)$$

$$E_t = M_A - \sqrt{(-\mathbf{p}_t)^2 + (M_A - m_N + E)^2}. \quad (11)$$

Here,  $d\sigma_{\pi^- p \rightarrow \eta' n}[\sqrt{s}, < m_{\eta'}^*, >, m_n, \mathbf{p}_{\eta'}]/d\mathbf{p}_{\eta'}$  is the off-shell inclusive differential cross section for the production of  $\eta'$  meson and neutron with reduced mass  $< m_{\eta'}^*, >$  and free mass  $m_n$ , respectively, and  $\eta'$  meson with in-medium momentum  $\mathbf{p}_{\eta'}$  in reaction (1) at the  $\pi^- p$  center-of-mass energy  $\sqrt{s}$ ;  $E_{\pi^-}$  and  $\mathbf{p}_{\pi^-}$  are the total energy and momentum of the incident pion ( $E_{\pi^-} = \sqrt{m_{\pi}^2 + \mathbf{p}_{\pi^-}^2}$ ,  $m_{\pi}$  is the free space pion mass);  $\rho(\mathbf{r})$  and  $P_A(\mathbf{p}_t, E)$  are the local nucleon density and the spectral function of the target nucleus A normalized to unity;  $\mathbf{p}_t$  and  $E$  are the internal momentum and removal energy of the struck target proton involved in the collision process (1);  $\sigma_{\pi^- N}^{\text{tot}}$  is the total cross section of the free  $\pi^- N$  interaction<sup>4)</sup>;  $Z$  and  $A$  are the numbers of protons and nucleons in the target nucleus, and  $M_A$  and  $R$  are its mass and radius; and  $\theta_{\eta'}$  is the polar angle of vacuum momentum  $\mathbf{p}_{\eta'}$  in the laboratory system with z-axis directed along the momentum  $\mathbf{p}_{\pi^-}$  of the initial pion. Since the momenta of the outgoing neutrons in reaction (1) are substantially greater than the typical average Fermi momentum of  $\sim 250$  MeV/c of the target nucleus, we neglect the correction of Eq. (9) for the Pauli blocking, leading to suppression of the available phase space.

For the nuclear density  $\rho(\mathbf{r})$  in the cases of the  $^{12}\text{C}$  and  $^{184}\text{W}$  target nuclei considered, we have employed, respectively, the harmonic oscillator and the Woods-Saxon distributions [13]:

$$\rho(\mathbf{r}) = \rho_N(\mathbf{r})/A = \frac{(b/\pi)^{3/2}}{A/4} \left\{ 1 + \left[ \frac{A-4}{6} \right] br^2 \right\} \exp(-br^2), \quad (12)$$

<sup>4)</sup>We use in the subsequent calculations the value of  $\sigma_{\pi^- N}^{\text{tot}} = 35$  mb for the incident pion momentum of 1.7 GeV/c [13].

$$\rho(\mathbf{r}) = \rho_0 \left[ 1 + \exp \left( \frac{r - R_{1/2}}{a} \right) \right]^{-1}, \quad (13)$$

where  $b = 0.355 \text{ fm}^{-2}$ ,  $R_{1/2} = 6.661 \text{ fm}$  and  $a = 0.55 \text{ fm}$ . For the  $\eta'$  production calculations in the case of the  $^{12}\text{C}$  target nucleus the nuclear spectral function  $P_A(\mathbf{p}_t, E)$  was taken from Ref. [18]. For the  $^{184}\text{W}$  target nucleus its single-particle part was assumed to be the same as that for  $^{208}\text{Pb}$  [19]. This latter was taken from Ref. [20]. The correlated part of the spectral function for  $^{184}\text{W}$  was taken from Ref. [18].

Following Ref. [14], we assume that the off-shell inclusive differential cross section  $d\sigma_{\pi^-p \rightarrow \eta' n}[\sqrt{s}, < m_{\eta'}^* >, m_n, \mathbf{p}'_{\eta'}]/d\mathbf{p}'_{\eta'}$  for  $\eta'$  creation in reaction (1) is equivalent to the respective on-shell cross section calculated for the off-shell kinematics of this reaction as well as for the final  $\eta'$  and neutron in-medium mass  $< m_{\eta'}^* >$  and free mass  $m_n$ , respectively. Taking into account Eq. (16) from Ref. [14], we get the following expression for the elementary in-medium differential cross section  $d\sigma_{\pi^-p \rightarrow \eta' n}[\sqrt{s}, < m_{\eta'}^* >, m_n, \mathbf{p}'_{\eta'}]/d\mathbf{p}'_{\eta'}$ :

$$\begin{aligned} \frac{d\sigma_{\pi^-p \rightarrow \eta' n}[\sqrt{s}, < m_{\eta'}^* >, m_n, \mathbf{p}'_{\eta'}]}{d\mathbf{p}'_{\eta'}} &= \frac{\pi}{I_2[s, < m_{\eta'}^* >, m_n] E'_{\eta'}} \\ &\times \frac{d\sigma_{\pi^-p \rightarrow \eta' n}(\sqrt{s}, < m_{\eta'}^* >, m_n, \theta_{\eta'}^*)}{d\Omega_{\eta'}^*} \\ &\times \frac{1}{(\omega + E_t)} \delta \left[ \omega + E_t - \sqrt{m_n^2 + (\mathbf{Q} + \mathbf{p}_t)^2} \right], \end{aligned} \quad (14)$$

where

$$I_2[s, < m_{\eta'}^* >, m_n] = \frac{\pi}{2} \frac{\lambda[s, (< m_{\eta'}^* >)^2, m_n^2]}{s}, \quad (15)$$

$$\lambda(x, y, z) = \sqrt{[x - (\sqrt{y} + \sqrt{z})^2][x - (\sqrt{y} - \sqrt{z})^2]}, \quad (16)$$

$$\omega = E_{\pi^-} - E'_{\eta'}, \quad \mathbf{Q} = \mathbf{p}_{\pi^-} - \mathbf{p}'_{\eta'}. \quad (17)$$

Here,  $d\sigma_{\pi^-p \rightarrow \eta' n}(\sqrt{s}, < m_{\eta'}^* >, m_n, \theta_{\eta'}^*)/d\Omega_{\eta'}^*$  is the off-shell differential cross section for the production of  $\eta'$  mesons with mass  $< m_{\eta'}^* >$  in reaction (1) under the polar angle  $\theta_{\eta'}^*$  in the  $\pi^-p$  c.m.s., which is assumed to be isotropic in our calculations of  $\eta'$  meson creation in  $\pi^-A$  collisions from this reaction:

$$\frac{d\sigma_{\pi^-p \rightarrow \eta' n}(\sqrt{s}, < m_{\eta'}^* >, m_n, \theta_{\eta'}^*)}{d\Omega_{\eta'}^*} = \frac{\sigma_{\pi^-p \rightarrow \eta' n}(\sqrt{s}, \sqrt{s_{\text{th}}^*})}{4\pi}. \quad (18)$$

Here,  $\sigma_{\pi^-p \rightarrow \eta' n}(\sqrt{s}, \sqrt{s_{\text{th}}^*})$  is the “in-medium” total cross section of reaction (1) having the threshold energy  $\sqrt{s_{\text{th}}^*} = < m_{\eta'}^* > + m_n$ . In line with the above, it is equivalent to the vacuum cross section  $\sigma_{\pi^-p \rightarrow \eta' n}(\sqrt{s}, \sqrt{s_{\text{th}}})$ , in which the free threshold energy  $\sqrt{s_{\text{th}}} = m_{\eta'} + m_n = 1.897 \text{ GeV}$  is replaced by the in-medium threshold energy  $\sqrt{s_{\text{th}}^*}$ . For the free total cross section  $\sigma_{\pi^-p \rightarrow \eta' n}(\sqrt{s}, \sqrt{s_{\text{th}}})$  we have used the following parametrization suggested in Ref. [14]:

$$\sigma_{\pi^-p \rightarrow \eta' n}(\sqrt{s}, \sqrt{s_{\text{th}}}) = \begin{cases} 223.5 (\sqrt{s} - \sqrt{s_{\text{th}}})^{0.352} [\mu\text{b}] & \text{for } 0 < \sqrt{s} - \sqrt{s_{\text{th}}} \leq 0.354 \text{ GeV}, \\ 35.6 / (\sqrt{s} - \sqrt{s_{\text{th}}})^{1.416} [\mu\text{b}] & \text{for } \sqrt{s} - \sqrt{s_{\text{th}}} > 0.354 \text{ GeV}. \end{cases} \quad (19)$$

As shown in Fig. 1, the parametrization (19) (solid line) fits well the existing sets of experimental data [21] for  $\pi^-p \rightarrow \eta' n$  (full triangles) and  $\pi^+n \rightarrow \eta' p$  (full circles) reactions. Looking at this figure, one can see that the cross section  $\sigma_{\pi^-p \rightarrow \eta' n}$  amounts approximately to  $110 \mu\text{b}$  for the initial pion momentum of  $1.7 \text{ GeV}/c$ . It is worth noting that for this momentum the cross section  $\sigma_{\pi^-p \rightarrow \eta' n}$  is

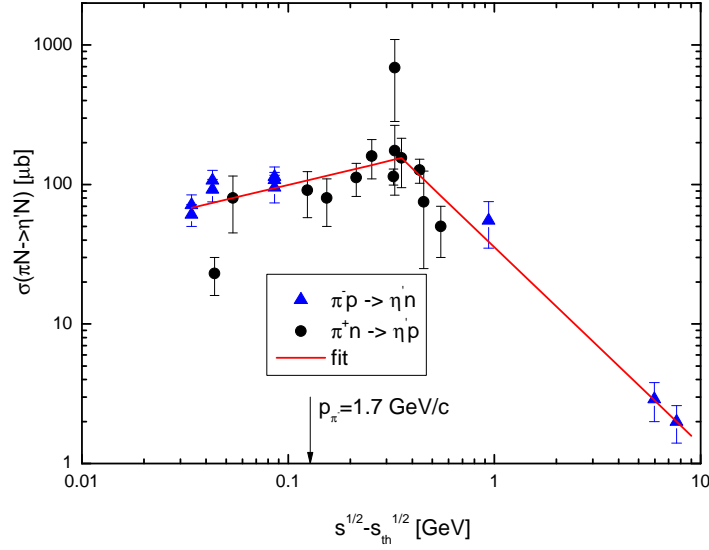


Figure 1: (color online) The total cross sections for the reactions  $\pi^-p \rightarrow \eta'n$  and  $\pi^+n \rightarrow \eta'p$  as functions of the excess energy  $\sqrt{s} - \sqrt{s_{\text{th}}}$ . The arrow indicates the excess energy  $\sqrt{s} - \sqrt{s_{\text{th}}} = 128$  MeV corresponding to the incident pion momentum of 1.7 GeV/c and a free target nucleon at rest.

larger by about two orders of magnitude than the total cross section  $\sigma_{\gamma N \rightarrow \eta' N}$  for  $\eta'$  photoproduction off the nucleon at incident photon energies around 2 GeV [3, 22, 23], studied in the CBELSA/TAPS  $\eta'$  photoproduction experiments [3–5]. Therefore, the collected statistics in pion-induced  $\eta'$  meson production experiment at beam momentum of 1.7 GeV/c is expected to be essentially higher than in the above experiments. This offers the possibility to investigate the  $\eta'$  effective scalar potential depth at substantially lower  $\eta'$  momenta ( $\sim 200$ – $300$  MeV/c) compared to those, studied in the experiments [3–5], via the measurements of the  $\eta'$  momentum distributions in  $\pi^-A$  reactions at modern experimental facilities such as the GSI pion beam facility and J-PARC.

In Eqs. (6)–(8) we assume that the direction of the three-momentum of the  $\eta'$  meson remains unchanged as it propagates from its production point inside the nucleus in the rather weak nuclear mean-field, considered in this paper, to the vacuum outside the nucleus. In this case, the quantities  $\langle d\sigma_{\pi^-p \rightarrow \eta'n}(\mathbf{p}_{\pi^-}, \mathbf{p}'_{\eta'})/d\mathbf{p}'_{\eta'} \rangle_A$  and  $d\mathbf{p}'_{\eta'}/d\mathbf{p}_{\eta'}$ , entering into Eq. (5), can be accounted for in our calculations as  $\langle d\sigma_{\pi^-p \rightarrow \eta'n}(p_{\pi^-}, p'_{\eta'}, \theta_{\eta'})/p_{\eta'}^2 dp'_{\eta'} d\Omega_{\eta'} \rangle_A$  and  $p'_{\eta'}/p_{\eta'}$ , where  $\Omega_{\eta'}(\theta_{\eta'}, \varphi_{\eta'}) = \mathbf{p}_{\eta'}/p_{\eta'}$ . Here,  $\varphi_{\eta'}$  is the azimuthal angle of the  $\eta'$  vacuum momentum  $\mathbf{p}_{\eta'}$  in the lab system. Similar to the  $\phi$  meson production in  $\pi^-A$  ( $A = {}^{12}\text{C}$  and  ${}^{184}\text{W}$ ) collisions at incident pion momentum of 1.7 GeV/c in the HADES experiment [9], we will consider the  $\eta'$  momentum distribution on these target nuclei in the acceptance window  $\Delta\Omega_{\eta'} = 10^\circ \leq \theta_{\eta'} \leq 45^\circ$  and  $0 \leq \varphi_{\eta'} \leq 2\pi$ . Integrating the full inclusive differential cross section (5) over this range, we can represent the differential cross section for  $\eta'$  meson production in  $\pi^-A$  collisions from the direct process (1), corresponding to the kinematical conditions of the HADES  $\phi$  meson production experiment [9], in the following form:

$$\begin{aligned} \frac{d\sigma_{\pi^-A \rightarrow \eta'X}^{(\text{prim})}(p_{\pi^-}, p_{\eta'})}{dp_{\eta'}} &= \int_{\Delta\Omega_{\eta'}} d\Omega_{\eta'} \frac{d\sigma_{\pi^-A \rightarrow \eta'X}^{(\text{prim})}(\mathbf{p}_{\pi^-}, \mathbf{p}_{\eta'})}{d\mathbf{p}_{\eta'}} p_{\eta'}^2 \\ &= 2\pi \left(\frac{Z}{A}\right) \left(\frac{p_{\eta'}}{p'_{\eta'}}\right) \int_{\cos 45^\circ}^{\cos 10^\circ} d\cos\theta_{\eta'} I_V[A, \theta_{\eta'}] \left\langle \frac{d\sigma_{\pi^-p \rightarrow \eta'n}(p_{\pi^-}, p'_{\eta'}, \theta_{\eta'})}{dp'_{\eta'} d\Omega_{\eta'}} \right\rangle_A. \end{aligned} \quad (20)$$

To get a better impression of the size of the effect of  $\eta'$  meson in medium mass shift on its yield in  $\pi^-C \rightarrow \eta'X$  and  $\pi^-W \rightarrow \eta'X$  reactions as well as of the strength of this yield in another laboratory  $\eta'$  emission polar angular ranges, we will also calculate the  $\eta'$  momentum distribution in these reactions with  $\eta'$  going into the laboratory solid angle  $\Delta\Omega_{\eta'}=0^\circ \leq \theta_{\eta'} \leq 10^\circ$  and  $0 \leq \varphi_{\eta'} \leq 2\pi$ .

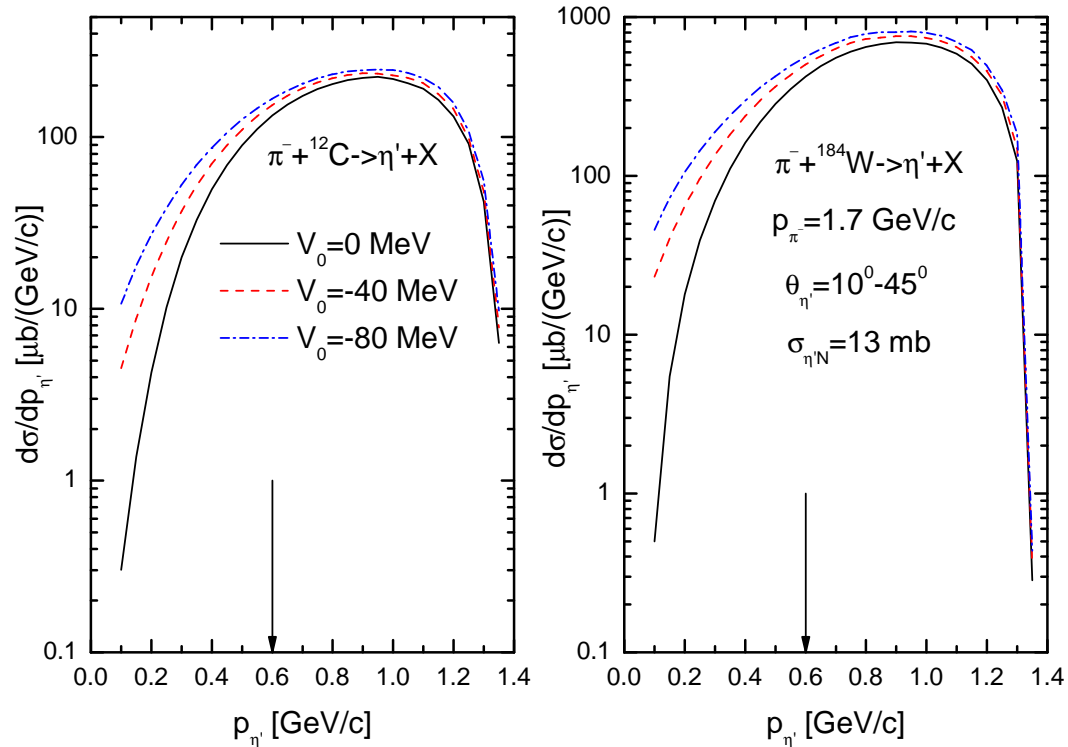


Figure 2: (color online) Momentum differential cross sections for the production of  $\eta'$  mesons from the primary  $\pi^-p \rightarrow \eta'n$  channel in the laboratory polar angular range of  $10^\circ$ – $45^\circ$  in the interaction of  $\pi^-$  mesons of momentum of 1.7 GeV/c with  $^{12}\text{C}$  (left panel) and  $^{184}\text{W}$  (right panel) nuclei for different values of the  $\eta'$  meson effective scalar potential  $V_0$  at density  $\rho_0$  indicated in the inset in the scenario with  $\sigma_{\eta'N} = 13$  mb. The arrows indicate the boundary between the low-momentum and high-momentum regions of 0.1–0.6 GeV/c and 0.6–1.35 GeV/c, respectively, of the  $\eta'$  spectra.

### 3 Results and discussion

First of all, we consider the momentum dependence of the absolute  $\eta'$  meson yield from the direct process (1). Figures 2 and 3 give momentum spectra of  $\eta'$  mesons produced in the interaction of 1.7 GeV/c  $\pi^-$  mesons with  $^{12}\text{C}$  and  $^{184}\text{W}$  nuclei at laboratory angles of  $10^\circ$ – $45^\circ$  and  $0^\circ$ – $10^\circ$ , respectively. In these figures, the curves – the respective momentum differential cross sections – represent the results of calculations on the basis of expression (20) for three values of the  $\eta'$  meson shift at a normal nuclear density: 0, -40, and -80 MeV in the scenario of collisional broadening of the  $\eta'$  meson characterized by the value of  $\sigma_{\eta'N} = 13$  mb. The absolute values of the differential cross sections show a rather wide variation for the mass shift range of  $V_0 = 0$  to -80 MeV in the low-momentum region of 0.1–0.6 GeV/c and especially at  $\eta'$  momenta  $\sim 0.2$ – $0.3$  GeV/c (where they have yet a measurable strength  $\sim 1$   $\mu\text{b}/(\text{GeV}/\text{c})$  and larger) for both target nuclei and for both laboratory polar  $\eta'$  production angular ranges of  $0^\circ$ – $10^\circ$  and  $10^\circ$ – $45^\circ$ .

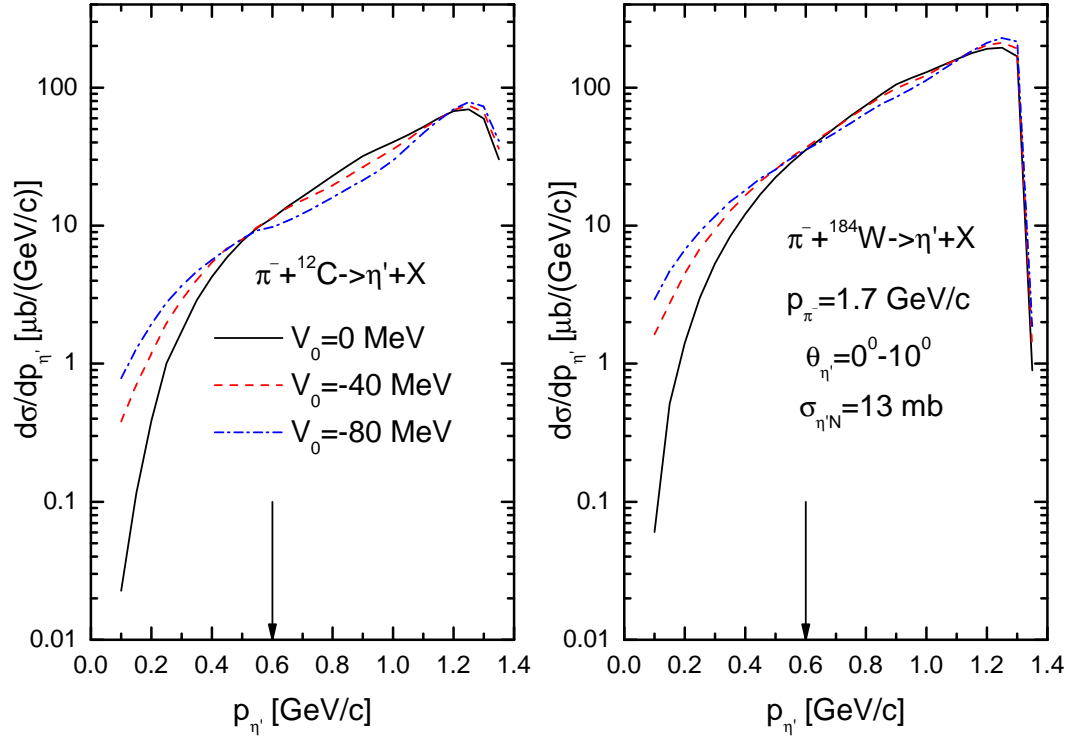


Figure 3: (color online) Momentum differential cross sections for the production of  $\eta'$  mesons from the primary  $\pi^- p \rightarrow \eta' n$  channel in the laboratory polar angular range of  $0^\circ$ – $10^\circ$  in the interaction of  $\pi^-$  mesons of momentum of 1.7 GeV/c with  $^{12}\text{C}$  (left panel) and  $^{184}\text{W}$  (right panel) nuclei for different values of the  $\eta'$  meson effective scalar potential  $V_0$  at density  $\rho_0$  indicated in the inset in the scenario with  $\sigma_{\eta'N} = 13$  mb. The arrows indicate the boundary between the low-momentum and high-momentum regions of 0.1–0.6 GeV/c and 0.6–1.35 GeV/c, respectively, of the  $\eta'$  spectra.

More detailed information about the sensitivity of the cross sections to the  $\eta'$  mass shift is contained in Fig. 4, where we show the momentum dependence of the ratio <sup>5)</sup> between the differential cross sections for  $\eta'$  production on  $^{12}\text{C}$  and  $^{184}\text{W}$  target nuclei, calculated for different values for  $\eta'$  mass shift at saturation density and presented in Figs. 2, 3, and the respective differential cross section, determined without this shift. One can see that at low ( $\sim 0.2$ – $0.3$  GeV/c)  $\eta'$  momenta there are sizeable and experimentally distinguishable differences between the options  $V_0 = 0$  MeV,  $V_0 = -40$  MeV, and  $V_0 = -80$  MeV for  $\eta'$  in-medium mass shift for all considered target nuclei and laboratory polar  $\eta'$  production angular domains. Thus, the  $\eta'$  momentum distributions are enhanced at mass shift  $V_0 = -40$  MeV by about a factor of 2.4 as compared to those obtained without this shift at momentum of 0.25 GeV/c. When going from  $V_0 = -40$  MeV to  $V_0 = -80$  MeV, the corresponding enhancement factor is of about 1.5 at this  $\eta'$  momentum. Accounting for the above enhancement factors, one may hope that even smaller mass shifts ( $V_0 \sim -20$  MeV) will probably be also experimentally accessible via the measurements of low-momentum parts of  $\eta'$  spectra in near-threshold  $\pi^- A$  interactions.

As also seen from Figs. 2 and 3, the  $\eta'$  production cross section at laboratory angles of  $\theta_{\eta'} = 10^\circ$ – $45^\circ$  and  $\eta'$  momenta  $\sim 0.2$ – $0.3$  GeV/c is greater than that at  $\eta'$  emission angles of  $\theta_{\eta'} = 0^\circ$ – $10^\circ$  for

<sup>5)</sup>We remind that a comparison of a similar differential cross section ratio calculated at various values of the  $\eta'$  in-medium mass shift with data on  $\eta'$  photoproduction off C and Nb nuclei was used in [3, 4] to extract this shift at a normal nuclear density.



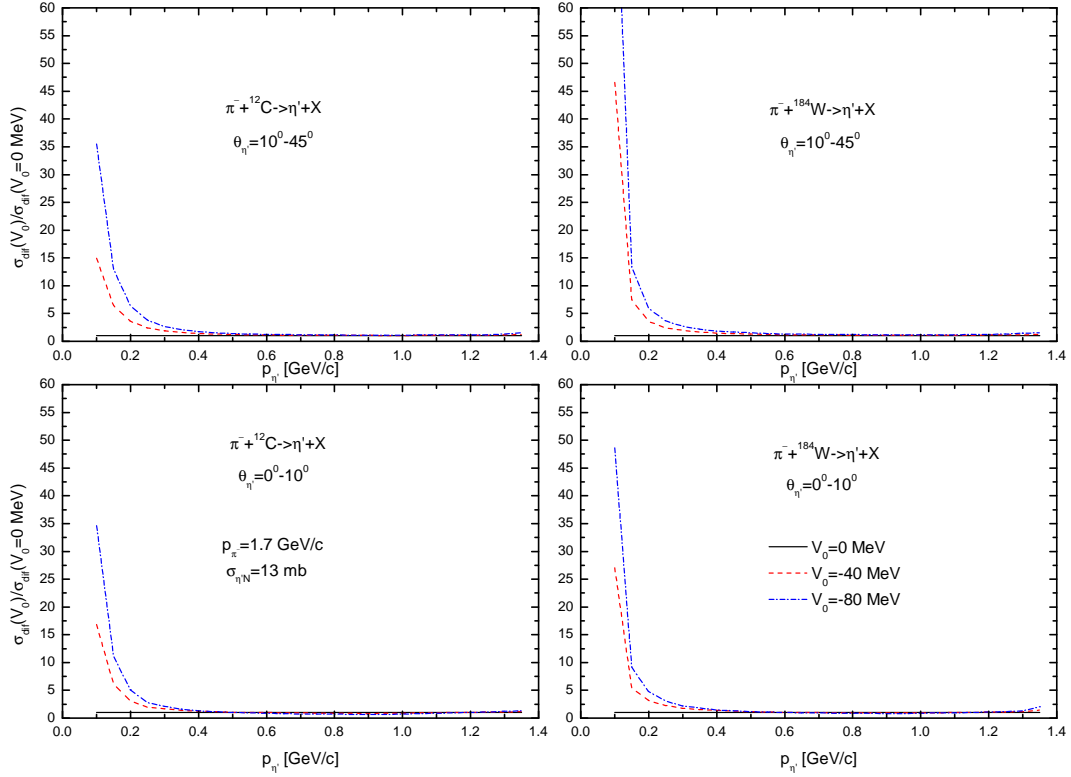


Figure 4: (color online) Ratio between the differential cross sections of  $\eta'$  production on C and W target nuclei as a function of the  $\eta'$  momentum at  $\eta'$  laboratory angles  $10^\circ$ – $45^\circ$  (upper two panels) and  $0^\circ$ – $10^\circ$  (lower two panels) by 1.7 GeV/c  $\pi^-$  mesons in primary  $\pi^- p \rightarrow \eta' n$  reactions proceeding on off-shell target protons, calculated with and without the  $\eta'$  in-medium mass shift, with values shown in the inset, in the scenario with  $\sigma_{\eta'N} = 13$  mb.

these momenta by about one order of magnitude. This makes the measurement of  $\eta'$  with momenta  $\sim 0.2$ – $0.3$  GeV/c in  $\pi^- A$  reactions for initial momentum of 1.7 GeV/c, for example, at GSI pion beam facility, using the HADES spectrometer <sup>6)</sup>, with aim of distinguishing at these momenta at least between zero, weak ( $V_0 \sim -40$  MeV) and relatively weak ( $V_0 \sim -80$  MeV)  $\eta'$  mass shifts (or  $\eta'$  effective scalar potentials) in cold nuclear matter quite promising. It is interesting to note that the model differential cross sections for  $\eta'$  photoproduction off  $^{12}\text{C}$  nucleus, adopted in Ref. [3] for extracting the  $\eta'$  scalar potential  $V_0$ , are less than those presented in Fig. 2 (left) by about two orders of magnitude at momenta  $\sim 0.2$ – $0.3$  GeV/c. This implies that the differential cross sections for  $\eta'$  production in  $\pi^- A$  collisions can be measured at these momenta with a substantially

<sup>6)</sup>In the CBELSA/TAPS  $\eta'$  photoproduction experiments [3–6]  $\eta'$  mesons were identified via the  $\eta' \rightarrow \pi^0 \pi^0 \eta \rightarrow \pi^0 \pi^0 \gamma \gamma \rightarrow 6\gamma$  decay chains with a branching ratio of 8.5 %. The measurement of  $\eta'$  mesons at HADES has only recently become possible. So far, HADES spectrometer could only detect charged particles, but recently an electromagnetic calorimeter was added to allow for the detection of photons. Thus, detection of  $\eta'$  mesons has become possible here [24]. At HADES one would probably identify the  $\eta'$  meson via the decay  $\eta' \rightarrow \pi^+ \pi^- \eta \rightarrow \pi^+ \pi^- \gamma \gamma$  with a branching ratio of 16.6 %. An alternative decay mode which may be easier experimentally because of the lower background could be  $\eta' \rightarrow \pi^+ \pi^- \eta \rightarrow \pi^+ \pi^- \pi^+ \pi^- \pi^0 \rightarrow 2\pi^+ 2\pi^- 2\gamma$  with a branching ratio of 11.9 % [24].

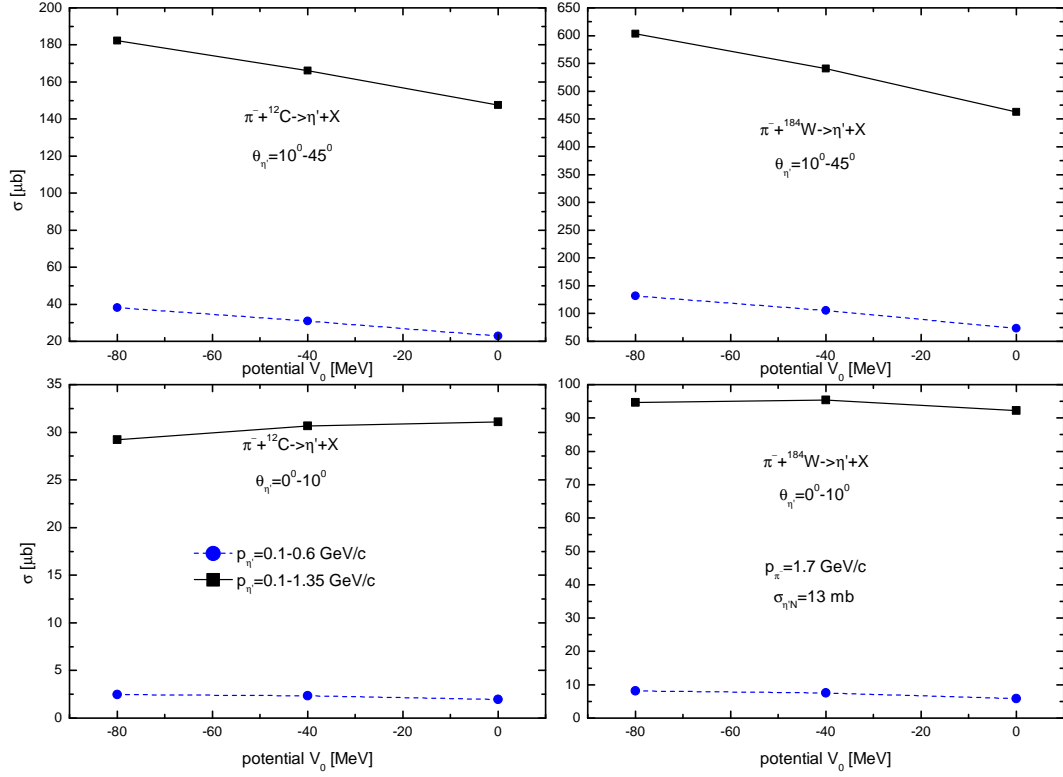


Figure 5: (color online) The total cross sections for the production of  $\eta'$  mesons from the primary  $\pi^-p \rightarrow \eta'n$  channel on C and W target nuclei with momenta of 0.1–0.6 GeV/c and 0.1–1.35 GeV/c in the laboratory polar angular ranges of  $10^\circ$ – $45^\circ$  (upper two panels) and  $0^\circ$ – $10^\circ$  (lower two panels) by 1.7 GeV/c  $\pi^-$  mesons in the scenario with  $\sigma_{\eta'N} = 13$  mb as functions of the effective scalar  $\eta'$  potential  $V_0$  at normal nuclear density. The lines are to guide the eye.

higher accuracy than that reached in the experiments [3, 4]. This would definitely permit evaluating the  $\eta'$  scalar potential  $V_0$  at  $\eta'$  momenta  $\sim 0.2$ – $0.3$  GeV/c in these collisions.

The sensitivity of the strength of the low-momentum parts of the  $\eta'$  spectra to the scalar potential  $V_0$ , shown in Figs. 2, 3, can be exploited to infer the correlation between the above strength and this potential from such integral measurements as the measurements of the total cross sections for  $\eta'$  production in  $\pi^-^{12}\text{C}$  and  $\pi^-^{184}\text{W}$  collisions by 1.7 GeV/c pions in the low-momentum (0.1–0.6 GeV/c) and full-momentum (0.1–1.35 GeV/c) regions. These cross sections, calculated for the  $\eta'$  laboratory polar angular domains of  $0^\circ$ – $10^\circ$  and  $10^\circ$ – $45^\circ$  by integrating Eq. (20) over the  $\eta'$  momentum  $p_{\eta'}$  in these regions in the scenario with  $\sigma_{\eta'N} = 13$  mb, as functions of the potential  $V_0$  are shown in Fig. 5. It is seen from this figure that due to larger cross sections and higher sensitivity to this potential the  $\eta'$  polar angular domain of  $10^\circ$ – $45^\circ$  is more favorable than the forward  $\eta'$  production polar angular range of  $0^\circ$ – $10^\circ$ . In this angular domain the highest sensitivity of the  $\eta'$  production cross section to the scalar potential  $V_0$  is observed, as was expected, in the low-momentum region of 0.1–0.6 GeV/c. Thus, for example, the  $\eta'$  total cross section is enhanced here at  $V_0 = -80$  MeV by a factor of about 1.8 compared to that obtained in the scenario with zero  $\eta'$  potential. Whereas, in the full  $\eta'$  momentum range of 0.1–1.35 GeV/c the respective enhancement

factor is about 1.3. Therefore, a comparison of the above "integral" results with the experimentally determined total  $\eta'$  creation cross sections in the low-momentum region of 0.1–0.6 GeV/c will also allow one to get the definite information about the average effective scalar potential  $V_0$  (or about the  $\eta'$  in-medium mass shift) at normal nuclear matter density  $\rho_0$  in this region.

Accounting for the above consideration, we come to the conclusion that the near-threshold  $\eta'$  momentum distribution and  $\eta'$  total cross section measurements at momenta  $\sim 0.2$ –0.3 GeV/c and 0.1–0.6 GeV/c, respectively, in  $\pi^-A$  reactions might permit to shed light on the possible  $\eta'$  in-medium mass shift (or on the scalar  $\eta'$ –nucleus optical potential) at these momenta. Such measurements could be performed in the future at the GSI pion beam facility or at J-PARC <sup>7)</sup>.

## 4 Conclusions

Our present study was aimed at studying the possibility of extracting information about the in-medium change of the  $\eta'$  meson mass (or about the effective  $\eta'$  scalar nuclear potential) at low meson momenta. For this, we have calculated the differential and total cross sections for  $\eta'$  production off carbon and tungsten nuclei at laboratory angles of 0°–10° and 10°–45° by  $\pi^-$  mesons with momentum of 1.7 GeV/c, which is close to the threshold momentum for  $\eta'$  meson production off the free target proton at rest. We have performed these calculations on the basis of the first-collision model, which describes incoherent  $\eta'$  meson creation in single collisions of incident  $\pi^-$  mesons with intranuclear target protons and takes into account three different options for its in-medium mass shift at saturation density  $\rho_0$ . The intrinsic properties of  $^{12}\text{C}$  and  $^{184}\text{W}$  target nuclei have been described in terms of their spectral functions, which account for the momenta of target protons and the energies of their separation from the nuclei. An inspection of the results of these calculations has shown that the present  $\eta'$  production cross sections are larger than those, studied in Ref. [3] in the  $\eta'$  photoproduction reactions, by about two orders of magnitude. At the same time, the calculations have shown that the high absolute values of the differential and total  $\eta'$  pion-induced production cross sections in the momentum ranges of 0.2–0.3 GeV/c and 0.1–0.6 GeV/c, respectively, possess a high sensitivity to changes in the in-medium shift of the  $\eta'$  mass. This offers the possibility of evaluating the above shift at these momenta from the respective data, which could be taken in future experiments at the GSI pion beam facility or at J-PARC.

## Acknowledgments

The author gratefully acknowledges Volker Metag for careful reading of the manuscript and valuable comments on it, improving its quality.

## References

- [1] V. Metag, M. Nanova, and E. Ya. Paryev, *Prog. Part. Nucl. Phys.* **97**, 199 (2017).
- [2] S. D. Bass and P. Moskal, arXiv:1810.12290 [hep-ph].
- [3] M. Nanova *et al.* (CBELSA/TAPS Collaboration), *Phys. Lett. B* **727**, 417 (2013).
- [4] M. Nanova *et al.* (CBELSA/TAPS Collaboration), *Phys. Rev. C* **94**, 025205 (2016).

---

<sup>7)</sup>It should be pointed out that the  $(\pi^+, p)$  and  $(\pi^-, n)$  reactions were proposed earlier [25] for the experimental search of  $\eta'$ -nuclear bound states at J-PARC.

- [5] M. Nanova *et al.* (CBELSA/TAPS Collaboration), Eur. Phys. J. A **54**: 182 (2018).
- [6] S. Friedrich *et al.* (CBELSA/TAPS Collaboration), Eur. Phys. J. A **52**, 297 (2016).
- [7] Y. K. Tanaka *et al.*, Phys. Rev. Lett. **117**, 202501 (2016).
- [8] V. Metag *et al.* approved proposal ELSA/03–2012–BGO–OD.
- [9] J. Adamczewski-Musch *et al.* (HADES Collaboration), arXiv:1812.03728 [nucl-ex].
- [10] J. Adamczewski-Musch *et al.* (HADES Collaboration), Eur. Phys. J. A **53**: 188 (2017).
- [11] H. Fujioka, Acta Phys. Polon. **B41**, 2261 (2010).
- [12] K. Ozawa *et al.* Direct measurements of  $\omega$  mass modification in  $A(\pi^-, n)\omega X$  reaction and  $\omega \rightarrow \pi^0\gamma$  decays. Proposal for J-PARC, 2010;  
[http://j-parc.jp/NuclPart/pac\\_1007/pdf/KEK-J-PARC-PAC2010-08.pdf](http://j-parc.jp/NuclPart/pac_1007/pdf/KEK-J-PARC-PAC2010-08.pdf).
- [13] E. Ya. Paryev, Chinese Physics C, Vol. **42**, No. (8), 084101 (2018).
- [14] E. Ya. Paryev, J. Phys. G: Nucl. Part. Phys. **40**, 025201 (2013).
- [15] S. Sakai and D. Jido, Phys. Rev. C **88**, 064906 (2013).
- [16] C.-H. Lee *et al.*, Phys. Lett. B **412**, 235 (1997);  
Z. Rudy *et al.*, Eur. Phys. J. A **15**, 303 (2002).
- [17] E. Oset and A. Ramos, Phys. Lett. B **704**, 334 (2011).
- [18] S. V. Efremov and E. Ya. Paryev, Eur. Phys. J. A **1**, 99 (1998).
- [19] E. Ya. Paryev, Eur. Phys. J. A **9**, 521 (2000).
- [20] E. Ya. Paryev, Eur. Phys. J. A **7**, 127 (2000).
- [21] V. Flaminio *et al.*. Compilation of cross sections.  
I:  $\pi^+$  and  $\pi^-$  induced reactions. CERN–HERA **83–01** (1983).
- [22] V. Crede *et al.* (CBELSA/TAPS Collaboration), Phys. Rev. C **80**, 055202 (2009).
- [23] I. Jaegle *et al.* (CBELSA/TAPS Collaboration), Eur. Phys. J. A **47**, 11 (2011).
- [24] V. Metag, private communication (2019).
- [25] H. Nagahiro, S. Hirenzaki, E. Oset, A. Ramos, Phys. Lett. B **709**, 87 (2012).